Techniques for a Wind Energy System Integration with an Islanded Microgrid

Megha Goyal, Yuanyuan Fan, Arindam Ghosh*, and Farhad Shahnia
Department of Electrical and Computer Engineering
Curtin University
Perth 6102, Western Australia

ABSTRACT — This paper presents two different techniques of a wind energy conversion system (WECS) integration with an islanded microgrid (MG). The islanded microgrid operates in a frequency droop control where its frequency can vary around 50 Hz. The permanent magnet synchronous generator (PMSG) based variable speed WECS is considered, which converts wind energy to a low frequency ac power. Therefore it needs to be connected to the microgrid through a back to back (B2B) converter system. One way of interconnection is to synchronize the MG side converter with the MG bus at which it is connected. In this case, this converter runs at the MG frequency. The other approach is to bring back the MG frequency to 50 Hz using the isochronization concept. In this case, the MG side converter operates at 50 Hz. Both these techniques are developed in this paper. The proposed techniques are validated through extensive PSCAD/EMTDC simulation studies.

Keywords — Microgrid, diesel generator, droop control, isochronization, WECS.

I. INTRODUCTION

The notion of the smart grid is the incorporation of all technologies, topologies and approaches that benefit utilities and customers. A microgrid (MG) is a key component of smart grid. A MG is defined as the interconnection of several distributed generators (DGs) such as diesel generators (DGENs), micro turbines, gas turbines, wind farms, PV arrays and battery storage systems. A microgrid can be connected to or separated from the electricity grid [1].

*Corresponding Author: Tel: +61 402 784 635
Email: Arindam.ghosh@curtin.edu.au

The most common way to supply electricity to remote customers is with diesel generators [2]. However, power generation based on diesel fuel can be offset by wind energy. Wind resource is the most promising energy choice due to its enormous availability. The development of new technologies for renewable sources offers attractive economic and environmental merits for energy support [3]. In Canada, integration of wind energy in distribution network to meet energy requirement in rural and remote areas is growing rapidly [4]. In Ramea wind-diesel project, a wind generator is integrated with the diesel generators to supply an islanded system [4]. Various designing aspects are reported for diesel generators operating in conjunction with wind turbines and energy storage in [5]. The design methodology and analysis approach for unit sizing of an islanded wind-diesel system is developed in [6].

This research discusses the integration techniques of a variable speed wind system with an islanded microgrid. In [7], an integration of a doubly-fed induction generator (DFIG) based wind generator within microgrid is introduced. It focuses on variable droop control for DFIG to adjust the output power according to available wind power. The case study of Rhodes Island power system is investigated in [8]. It introduces a frequency controller for PMSG and DFIG types of wind turbines to regulate frequency in the islanded microgrid. In frequency droop control, frequency varies according to load variation. In literature, various kinds of droop control strategies have been proposed [9-11]. In [12], isochronous load sharing is discussed for inverter based distributed generation. In this, the inverter operates at constant set reference frequency regardless of load. However, load power measurement is required to achieve this.

The frequency regulation in an islanded microgrid using a wind power system is discussed in [13], where the frequency of the microgrid is maintained constant irrespective of load variation through wind system. The controller regulates power from the wind system according to load variation in the microgrid. Thus, the wind system is used only to maintain the microgrid frequency constant rather than using available renewable power to support the load.

In this paper, an optimal power control (OPC) scheme is used for maximum power point track (MPPT) in WECS. The PMSG based WECS is considered, which is connected to the microgrid through a back to back

(B2B) voltage source converter (VSC). This B2B converter is required to connect low frequency generator of the WECS to the microgrid which is operating around the set reference frequency of 50 Hz. This paper mainly focuses on integration techniques of WECS with an islanded microgrid. The islanded microgrid operates in frequency droop control. To integrate the WECS at the set reference frequency with the islanded microgrid, modified droop control with isochronous concept is proposed to maintain the system frequency constant with the load fluctuation and wind power variation. Moreover, another integration technique using synchronization concept is also presented in which isochronization is not required. Extensive digital computer simulation results using PSCAD/EMTDC are presented to validate the proposals.

II. SYSTEM STRUCTURE

The system considered has a microgrid with two diesel generators (DGENs) and a WECS that operates in MPPT. The diesel generator set consists of a 4-stroke internal combustion (IC) engine coupled to a synchronous generator. The IC engine speed is controlled through the fuel input rate by a speed governor. A PID controller is used in the governor to maintain output speed. The synchronous generator contains an exciter and an automatic voltage regulator (AVR). The AVR controls the field supply of the generator to maintain the required terminal voltage. Note that the reference speed (for governor) and generator terminal voltage (for AVR) are obtained from the frequency droop control. The WECS is connected to the microgrid through a back to back converter. The system data used are given in the Appendix. The BTB converter consists of two conventional voltage source converters (VSC-1 and VSC-2) connected through a common dc link capacitor. VSC-1 is used to control the power flow from the wind turbine, while VSC-2 is used to control the dc link capacitor voltage (V_{dc}) constant. The microgrid frequency varies within the droop limits according to the load variations. VSC-2 connected to the microgrid, should operate at the same frequency of the microgrid. To achieve this, two techniques are proposed: (1) synchronization of the VSC-2 voltage at the same frequency of the microgrid and (2) modifying the frequency droop control such that the microgrid always operates at the set reference frequency.

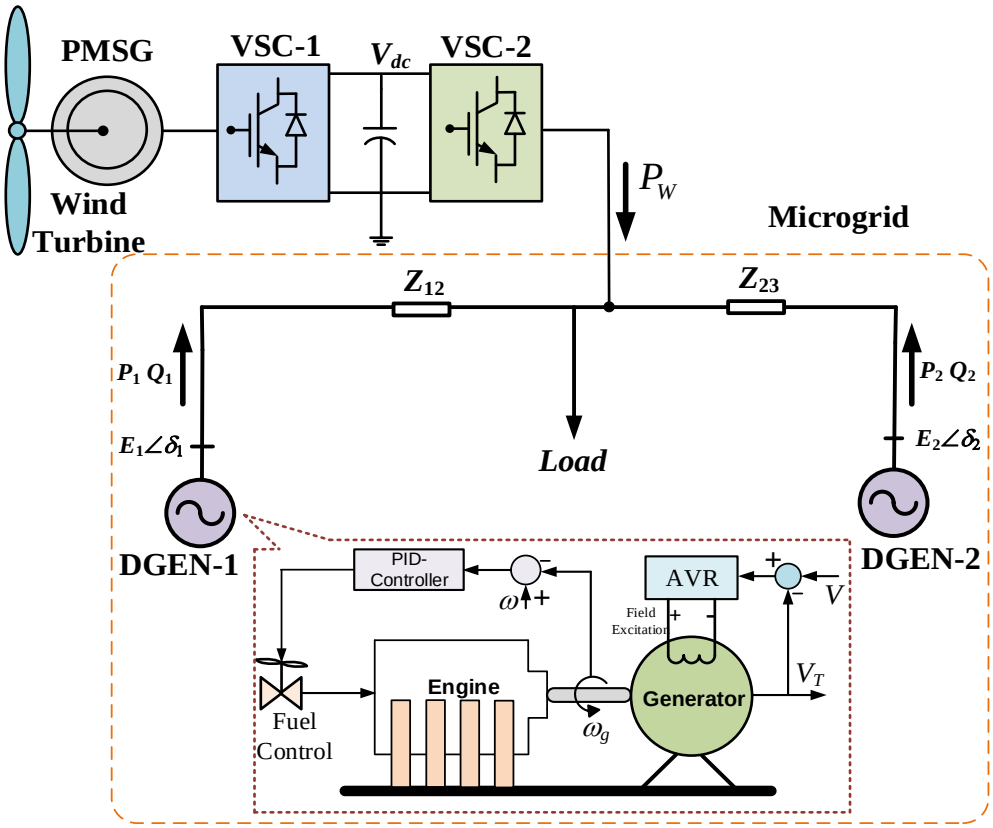

Fig. 1. System structure.

III. WIND ENERGY CONVERSION SYSTEM

A. Wind Turbine with PMSG Model

The wind power that is captured by the blade and converted into mechanical power can be calculated by [14]

$$P_M = \frac{1}{2}\rho A v_w^3 C_p \tag{1}$$

where ρ is the air density, A is the cross-sectional area through which the wind passes, v_w is the wind speed and C_p is the power coefficient of the blade. The rotor efficiency C_p is calculated from [15]

$$C_p = 0.5176\left(\frac{116}{\lambda_i} - 0.4\beta - 5\right)e^{\frac{-21}{\lambda_i}} + 0.0068\lambda \tag{2}$$

where β is the pitch angle, λ is the tip speed ratio (TSR), which is defined as the blade tip moving speed divided by the wind speed, and λ_i is given by [16]

$$\frac{1}{\lambda_i} = \frac{1}{\lambda + 0.08\beta} - \frac{0.035}{\beta^3 + 1} \tag{3}$$

The wind turbine operates at the generator control mode when the wind speed is below the rated wind speed, and works under the pitch control mode when the wind speed exceeds the rated value [17]. The parameters of the wind turbine and PMSG used are given in the Appendix.

B. PMSG Operation with Varied Wind Speeds

To verify the modelling and control strategy applied in this paper, the varied wind speeds are written as the following equations:

$$v_w = \begin{cases} v_m & t < t_1 \\ v_m + k \cdot (t - t_1) & t_1 < t < t_2 \\ v_m + k \cdot (t_2 - t_1) & t > t_2 \end{cases} \tag{4}$$

$$v_{ES} = k \cdot (t_2 - t_1) \tag{5}$$

where v_w is the wind speed available to the turbine, v_m is the mean wind speed, k is the ramp change in the wind speed, t_1 and t_2 are the starting and ending time respectively of the wind speed ramping duration, v_{ES} is the external wind speed of the wind source.

C. OPC Based MPPT for PMSG

The schematic diagram of the PMSG with B2B voltage source converters is shown in Fig. 2. The kinetic energy of the wind is converted into mechanical energy by the wind turbine and then transmitted to the generator. VSC-1 controls the active power through MPPT, while VSC-2 maintains the DC capacitor voltage constant.

To extract the maximum power from the wind energy, turbine blades should change their speed as the wind speed changes. Reference [18] gives out three methods to realize the MPPT control. Based on the PMSG model in this paper, to control the generator power, a method similar to Optimal Torque Control (OTC) is applied. This is called Optimal Power Control (OPC). The principle of the OTC is that the wind turbine mechanical torque T and the turbine speed ω_p have the following relationship at MPPT [18]

$$T \propto \omega_p^2 \tag{6}$$

Assuming that the generator power is denoted by P_g, which is given in OPC as

$$P_g \propto \omega_p^3 \tag{7}$$

It should be noted that the values of the turbine speed and the generator speed are equal, considering that the PMSG model is a direct drive. Besides, the generator mechanical torque is equal to its electromagnetic torque in the steady state. Equation (7) is the basis of OPC. Suppose

$$P_g = K_{opt} \times \omega_p^3 \tag{8}$$

where K_{opt} is calculated according to the generator rated parameters as

$$\begin{cases} K_{opt} = \dfrac{P^*}{(\omega_p^*)^3} \\ \omega_p^* = 2\pi \cdot \dfrac{f^*}{p} \end{cases} \tag{9}$$

In (9), P^*, ω_p^*, f^* and p are the rated power, rated speed, rated frequency and pole pairs of the generator.

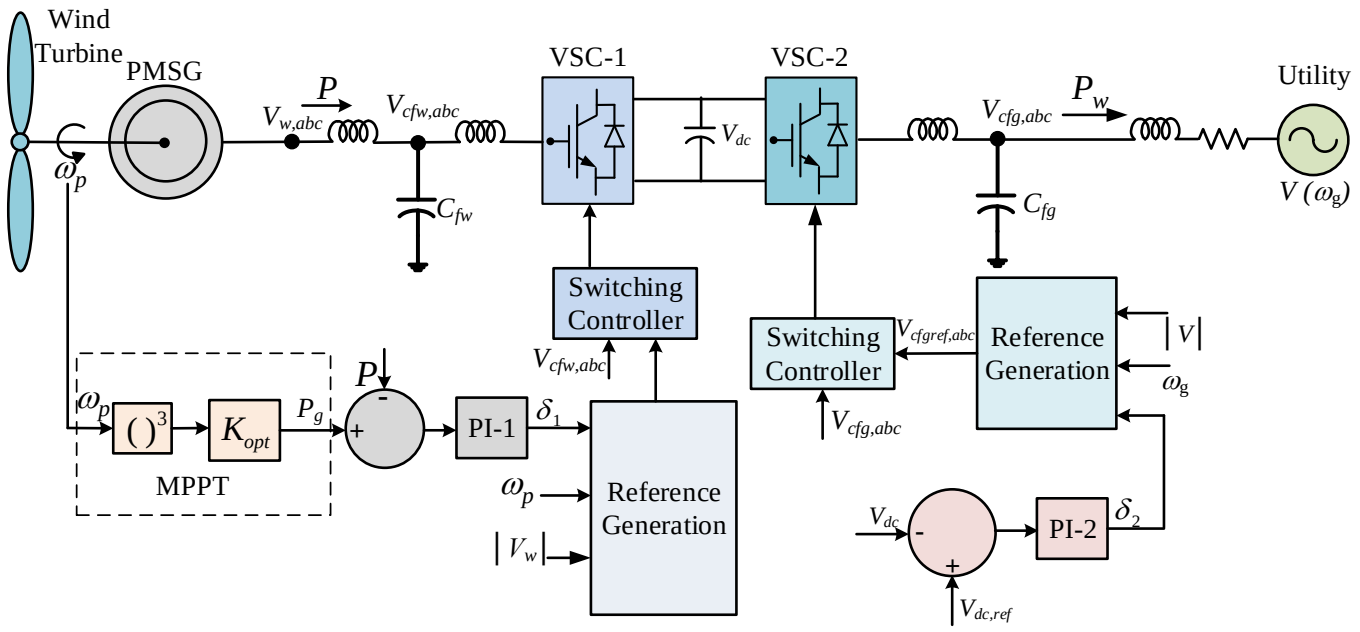

Fig. 2. Schematic diagram of wind energy conversion system

D. Control of B2B Converters

To control MPPT wind power flow to the microgrid, VSC-1 generates the voltage across the filter capacitor (C_{fw}) with an angle deviation from the PMSG output voltage. This power angle is calculated by a PI controller as

$$\delta_1 = K_{P1}\left(P_g - P\right) + K_{I1}\int\left(P_g - P\right)dt \tag{10}$$

where P_g is the wind power calculated from (8) and P is the actual power from the PMSG.

The purpose of the VSC-2 is to hold the voltage (V_{dc}) across the DC link capacitor constant. Note that this voltage will remain constant only when it neither supplies nor absorbs any real power. Therefore the power obtained from wind turbine should ideally appear at the grid side. However, this is not practical since the converter losses must also be supplied from the generated power. Therefore holding the capacitor voltage is tantamount to extracting the maximum possible power from the wind turbine after supplying the converter losses. For the DC voltage control another PI controller (PI-2) is designed, which is given by

$$\delta_2 = K_{P2}\left(V_{dc,ref} - V_{dc}\right) + K_{I2}\int\left(V_{dc,ref} - V_{dc}\right)dt \tag{11}$$

where $V_{dc,ref}$ is the reference dc capacitor voltage and V_{dc} is the actual dc capacitor voltage. K_{P2} and K_{I2} are proportional and integral gains of the controller respectively. The converters are controlled in a hysteresis band output feedback control as explained in [19].

To illustrate the operation of OPC based MPPT control, consider the WECS that is connected to an infinite bus (Fig. 2). The wind speed pattern is assumed as

$$t_1 = 3s, t_2 = 4s, k = 1, V_m = 10\ m/s$$

Fig. 3 (a) shows the wind speed variation pattern. In this the mean wind speed is 10 m/s, which ramps up between 3 s and 4 s to 11m/s. The power output of the WECS follows the same pattern of the wind speed, as can be seen from Fig. 3 (b). The TSR versus wind speed is shown in Fig. 3 (c), where the TSR is kept at its optimal value regardless of the change in wind speed. The small fluctuation that can be seen in TSR is due to the control of WSC, which cannot respond istantaneously because of the dynamics of its LC filters. The rotor

efficiency (C_p) against wind speed is plotted in Fig. 3 (d). It is also constant follwing the TSR. Figs. 3 (c) and (d) demonstrate that a stable maxium efficiency is being achieved when wind speed is varying. This indicates the effectiveness of the applied MPPT control. The WECS is connected with the utility. Therefore, VSC-2 operates at the fix frequency (ω_g) of the utility. When the WECS gets integrated with the MG, ω_g cannot remain constant. Therefore measures have to be taken to eliminate any system oscillation due to frequency mismatch.

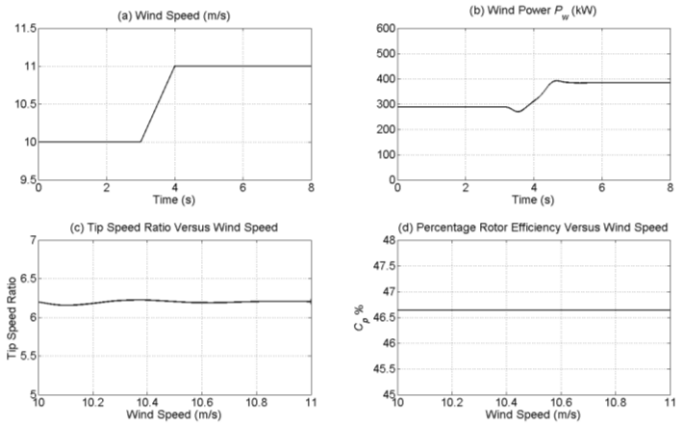

Fig. 3. Wind speed variation, output power, TSR and rotor efficiency.

IV. INTEGRATION OF WECS WITH MICROGRID

Since the microgrid operates in the frequency droop control, the frequency can vary within the limits of a frequency band. Therefore, VSC-2 must be synchronized with the microgrid frequency. As mentioned before, two techniques are proposed for the interconnection. These are discussed below.

A. Frequency Droop Control with Isochronization

In this technique, the frequency of the microgrid is held constant at 50 Hz by integrating isochronization with frequency droop control. Therefore, the VSC-2 can connect to the microgrid at the set reference frequency. In the islanded microgrid, the DGs operate in the conventional frequency droop control, given by

$$\omega = \omega^* + m \times (0.5 \times P^* - P) \tag{12}$$

where the instantaneous and rated frequency of the DGs are ω and ω^* respectively. The rated and measured real powers are represented by P^* and P respectively. The droop coefficient is denoted by m. The droop parameters

of all DGs in a microgrid depend on their respective ratings such that all of them operate at the same frequency in the steady state. How these droop parameters can be calculated has been explained in [20].

Equation (12) signifies that when the system frequency is rated (50 Hz), the DG should supply half of its rated power. The frequency will be below (above) 50 Hz when the DG supplies more (less) than half of its rated power. The droop gain is calculated based on a frequency limit of ± 0.3 Hz. In isochronous mode, the frequency of the microgrid must remain constant at 50 Hz. Therefore, if the droop control and isochronous mode are combined, the system can operate at the set reference frequency while sharing load power according to DG ratings.

To achieve this, the droop line shifts according to the load variation while preserving its slope. For constant droop coefficient, each DG has its own droop line according to its rating with the constant droop coefficient. The droop line shifts in such a way that it retains the same slope and can supply load power demand at the set reference frequency.

The droop lines of Fig. 4 are considered for one of the DGs. Ordinarily, the DG operates in line-1. This implies that when it supplies P_1, the frequency should be ω_1. However, it is required that the DG operates at 50 Hz (ω^*). Therefore the frequency must be compensated by the amount $\Delta\omega = \omega^* - \omega_1$. We also need to maintain the power sharing, which depends on the slope of the droop lines. Therefore the quantity $\Delta\omega$ must be kept zero against any frequency variation due to load change. To achieve this, a PID controller is used to set frequency variation to zero. This is shown in Fig. 5. The output of the PID controller is added to the output of the droop controller to produce ω_1', which is the input of the DGEN speed governor. Note that in steady state, $\omega_1' = \omega^*$. This means that the droop line is now shifted to line-2, which gives the power output of P_1 at ω^*.

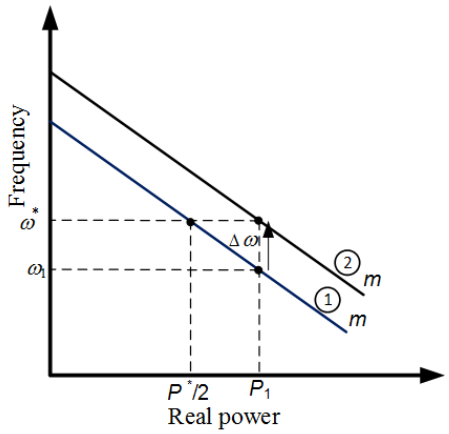

Fig. 4. Frequency droop control with isochronous mode.

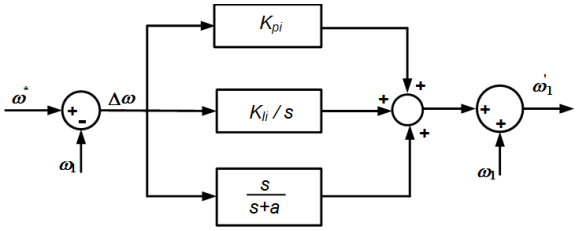

Fig. 5. Isochronous controller.

B. Synchronization with microgrid

In this technique, the microgrid operates in conventional frequency droop control and its frequency varies within the frequency band according to the load power demand. Therefore, to connect the WECS with the microgrid, VSC-2 must be synchronized with the microgrid to operate at the same frequency. To achieve this, a simple algorithm is used for synchronization, which is discussed below.

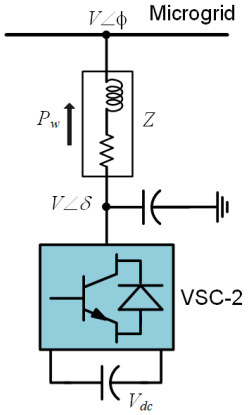

Fig. 6. VSC-2 connection with microgrid.

The frequency of the microgrid is set at ω. The instantaneous voltages at the point of connection of VSC-2 are given as

$$\begin{aligned} v_a &= V \times \sqrt{2}\sin(\omega t + \phi) \\ v_b &= V \times \sqrt{2}\sin(\omega t - 120° + \phi) \\ v_c &= V \times \sqrt{2}\sin(\omega t + 120° + \phi) \end{aligned} \tag{13}$$

Using symmetrical component theory [19], the positive sequence component of the instantaneous voltage of (13) will be

$$\begin{aligned} \mathbf{v}_{\mathbf{a1}} &= \left(v_a + v_b a + v_c a^2\right)/3 \\ &= \frac{V}{\sqrt{2}}\left[\sin(\omega t + \phi) - j\cos(\omega t + \phi)\right] \end{aligned} \tag{14}$$

$$\mathbf{v}_{\mathbf{a1}} = \frac{V}{\sqrt{2}}(\alpha + j\beta) \tag{15}$$

where $a = e^{j120°}$ and

$$\alpha = \sin(\omega t + \phi),\ \beta = -\cos(\omega t + \phi) \tag{16}$$

Note that from (11) δ_2 is obtained. The purpose is to add this angle with positive sequence voltage of (14). Therefore, the positive sequence of the reference voltage across the filter capacitor of VSC-2 is

$$\begin{aligned} V_{vsc2} &= \frac{V}{\sqrt{2}}\left[\sin(\omega t + \phi + \delta_2) - j\cos(\omega t + \phi + \delta_2)\right] \\ V_{vsc2} &= \frac{V}{\sqrt{2}}\left[\sin(\omega t + \phi)\cos\delta_2 + \cos(\omega t + \phi)\sin\delta_2\right. \\ &\qquad \left. - j\cos(\omega t + \phi)\cos\delta_2 + j\sin(\omega t + \phi)\sin\delta_2\right] \\ &= \frac{V}{\sqrt{2}}\left[(\alpha + j\beta)\cos\delta_2 - (\beta - j\alpha)\sin\delta_2\right] \end{aligned} \tag{17}$$

From (16) and (17), V_{vsc2} can be calculated. The instantaneous negative sequence is the complex conjugate of the positive sequence. Also, since the system is assumed to be balanced, the instantaneous zero sequence will be zero. Therefore, using inverse symmetrical component transform, the instantaneous reference voltages

across the capacitor are obtained. Thus VSC-2 can track this reference output voltage without any explicit frequency measurement.

V. SIMULATION STUDIES

Simulation studies are carried out in PSCAD/EMTDC to verify the discussed techniques above with different patterns of wind speed in WECS connected to the microgrid. The parameters of the considered system are given in the Appendix.

Three different case studies are considered. These are

(a) Nominal operation of the islanded microgrid

(b) WECS integration with the microgrid using isochronization

(c) WECS integration with the microgrid using frequency synchronization

***Case* (*a*)**: The considered 11kV microgrid consists of two DGENs with ratings of 500kW and 250kW respectively and its local load. The droop coefficients for each DG are calculated from their ratings. The local load is assumed to be 625 kW. As shown in Fig. 7 (a), both DGENs share the power in the ratio of 2:1 according to their ratings. The microgrid frequency is 49.8 Hz with the conventional droop control method as shown in Fig. 7 (b). The synchronization technique is applied at 2 s and it can be seen from Fig. 7 (b) that the frequency converges to 50 Hz. However the powers remain unaltered. Once the load power changes at 11 s, the power supplied by the DGs also changes in a same ratio, which is shown in Fig. 8 (a). However, in Fig. 8 (b), it can be seen that with the proposed method, the system retains at the set reference value of 50 Hz. This verifies that the system frequency maintains at the set reference with load power sharing according to the ratings of the DGs.

Case* (*b*):* The microgrid operates in frequency droop control with isochronous mode. Therefore, the microgrid operates at the set reference frequency and hence VSC- 2 can also operate at the same frequency. The results are discussed below.

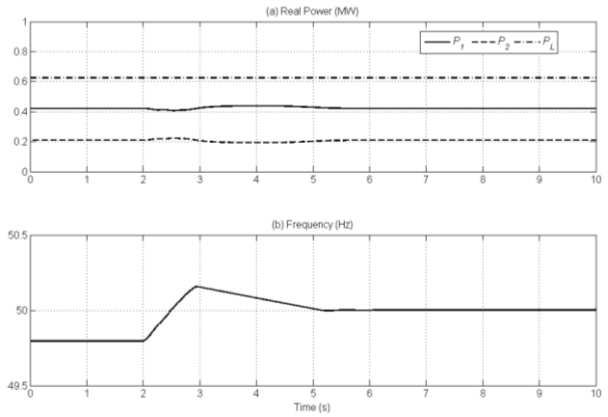

Fig. 7. Real power sharing and frequency of microgrid with conventional droop and isochronization in Case (a).

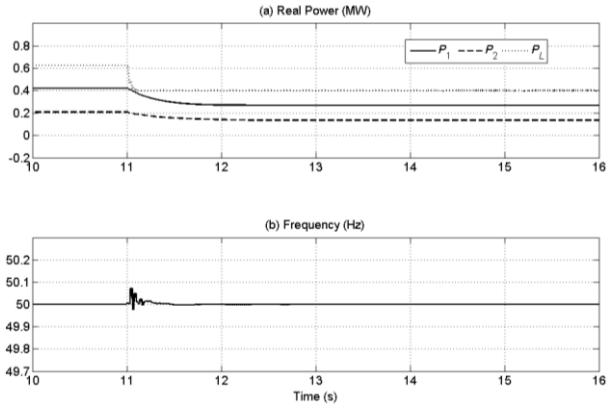

Fig. 8. Real power sharing and frequency with load variation in Case (a).

Case (*b.*1)*: Microgrid with constant speed WECS*

For this case, it has been assumed when the WECS system is connected to the microgrid at 2 s, the sources are operating in the steady state. The WECS supplies its total power to the microgrid. The real power flow in the microgrid is shown in Fig. 9 (a). It can be seen from this figure that the power supplied by the DGs reduces proportionally, maintaining the sharing ratio. The frequency of the microgrid is shown in Fig. 9 (b). It can be seen that the system frequency is retained at the set reference value of 50 Hz even after the integration of the WECS. The dc link capacitor voltage is shown in Fig. 10. It is held constant at 2.5 kV barring some transients by VSC-2 even after the WECS connects to the microgrid.

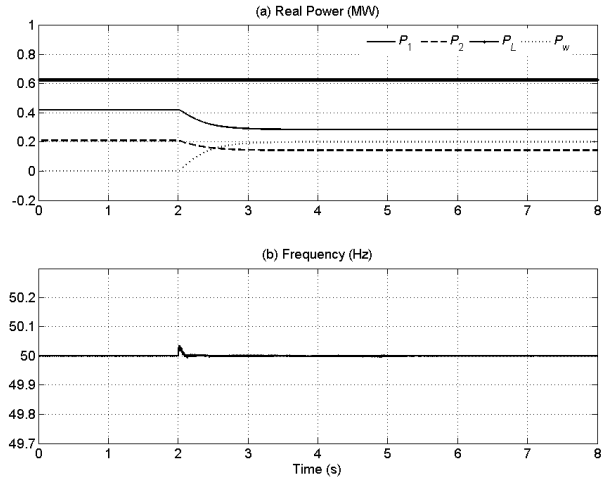

Fig. 9. Real power flow in microgrid with WECS and microgrid frequency in Case (b.1).

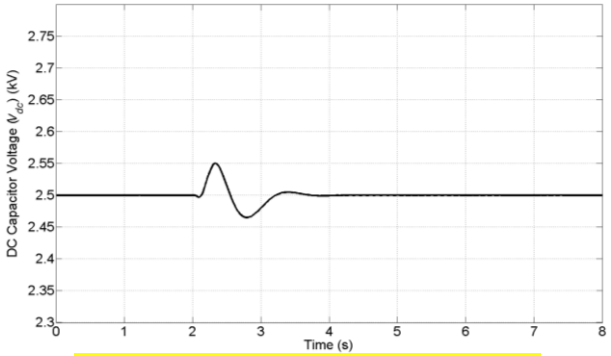

Fig. 10. DC capacitor voltage in Case (b.1).

Case (*b.*2)*: Microgrid with variable speed WECS*

In this case, the wind speed of the WECS is considered variable. As shown in Fig. 11, initially the wind speed is constant at 10 m/s. Then at 10 s, it starts ramping up to 12 m/s till 12 s. The output power of WECS also follows the pattern of the wind speed as shown in Fig. 12 (a). Once the wind speed increases, the output power of WECS also increases and therefore the power supplied by the DGENs reduces. The system frequency with the variation of the output power of the WECS is also maintained at the set reference value of 50 Hz as shown in Fig. 12 (b).

Case (*b.*3)*: Tripping of WECS*

Usually wind turbines start to operate when the wind speed exceeds 4-5 m/s, and are shut off at speeds over 25 to 30 m/s [14]. If wind speed is less than the cut in speed or higher than the cut off speed, WECS will be disconnected from the microgrid. In this case, the wind speed is reduced from 10 m/s to the cut in speed as

shown in Fig. 13. Therefore, the power P_W from WECS becomes zero after 11 s. It can be seen in Fig. 14 (a) that now load power is supplied only from the DGENs. Furthermore, the system frequency is retained constant at the set reference value as shown in Fig. 14 (b).

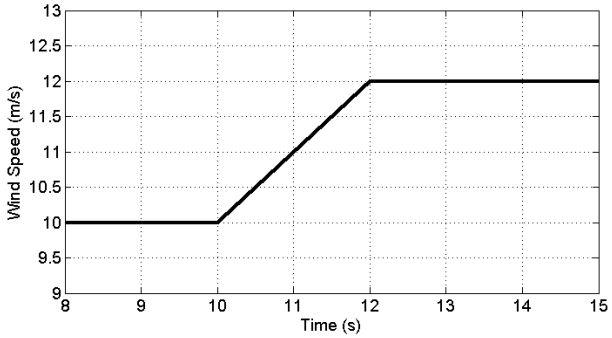

Fig. 11. Wind speed in Case (b.2).

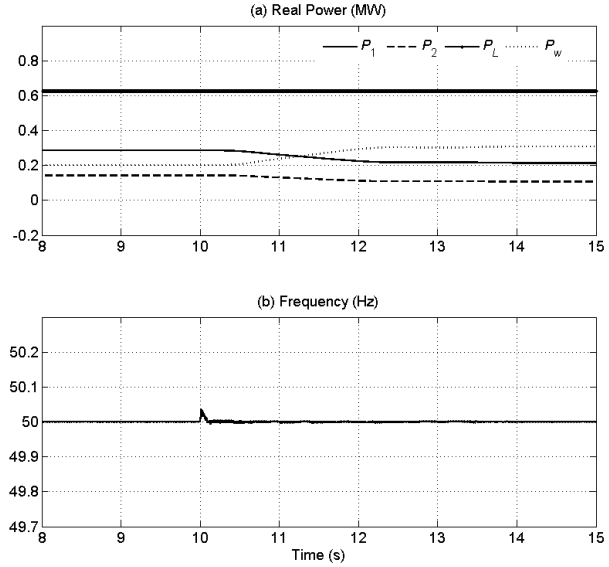

Fig. 12. Power flow in microgrid with WECS and microgrid frequency in Case (b.2).

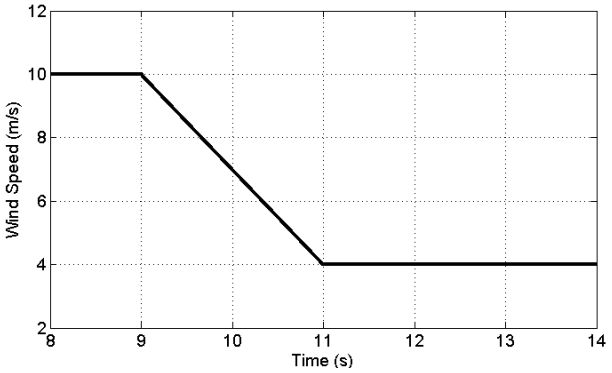

Fig. 13. Wind speed in Case (b.3).

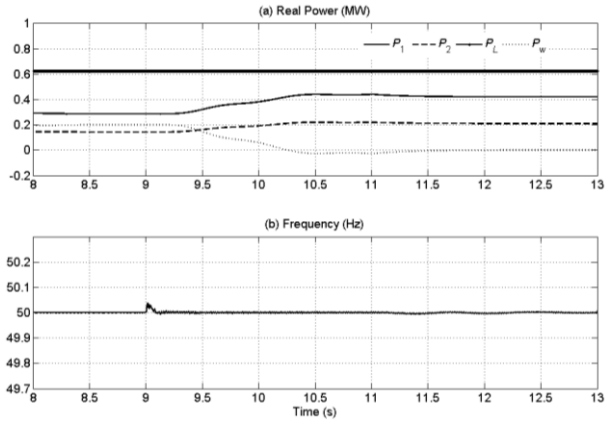

Fig. 14. Power flow in microgrid with WECS and frequency in Case (b.3).

***Case* (*c*)**: The microgrid operates in conventional frequency droop control and the frequency of the microgrid varies within the frquency band according to load variation. Therefore, for connecting the WECS with the microgrid, the synchronization algorithm is used. The simulation results are discussed below.

Case (*c*.1)*: Microgrid with constant speed WECS*

It is assumed that when WECS connects to the microgrid at 2 s, the wind speed is constant at 10 m/s. From Fig. 15 (a), it can be seen that the power supplied from the DGENs reduces and the system frequency also increases due to power reduction. This is shown in Fig. 15 (b). The dc capacitor voltage is held constant by VSC-2 during the connection of WECS with microgrid as shown in Fig. 16.

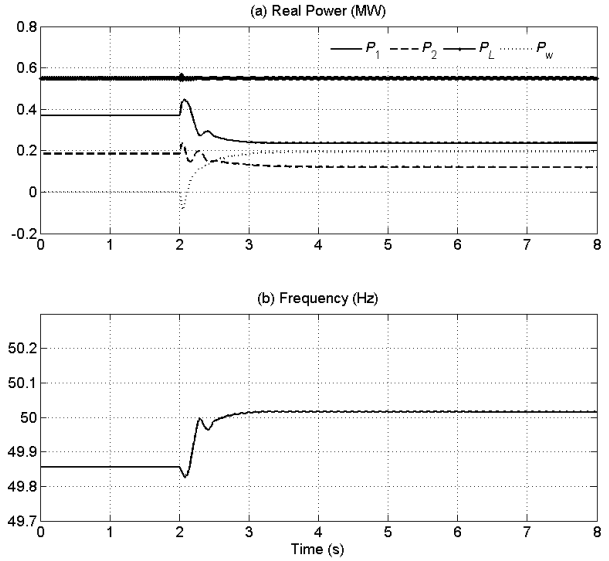

Fig. 15. Real power sharing and frequency of the microgrid in Case (c.1).

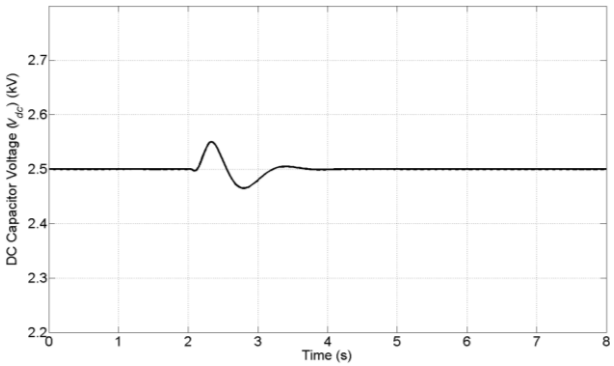

Fig. 16. DC capacitor voltage (V_{dc}) in Case (c.1).

It can be seen in Fig. 17 (a) that once the load is increased to 625 kW at 10 s, the power of DGENs increases in a same proportion and the power of WECS (P_w) is retained constant. The frequency of the microgrid also reduces as shown in Fig. 17 (b).

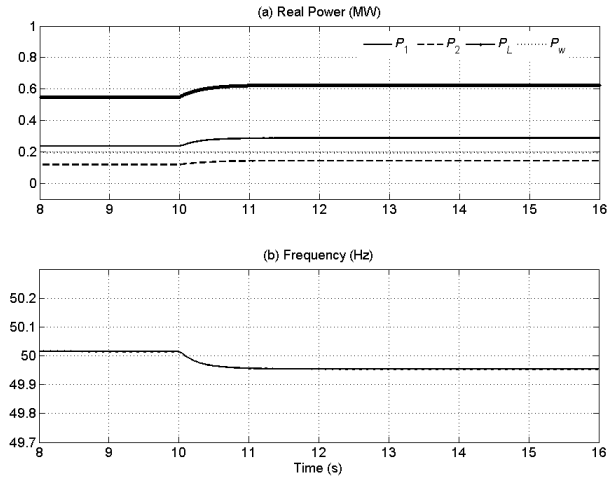

Fig. 17. Real power sharing and frequency of the microgrid with local load variation in Case (c.1).

Case (*c.*2)*: Microgrid with variable speed WECS*

In this case, it is assumed that the wind speed ramps up from 10 m/s to 11 m/s. The power flow from the WECS follows the wind speed pattern and the powers of DGENs reduce according to the available WECS power and load requirement. This is shown in Fig. 18 (a). The variation in microgrid frequency is shown in Fig. 18 (b).

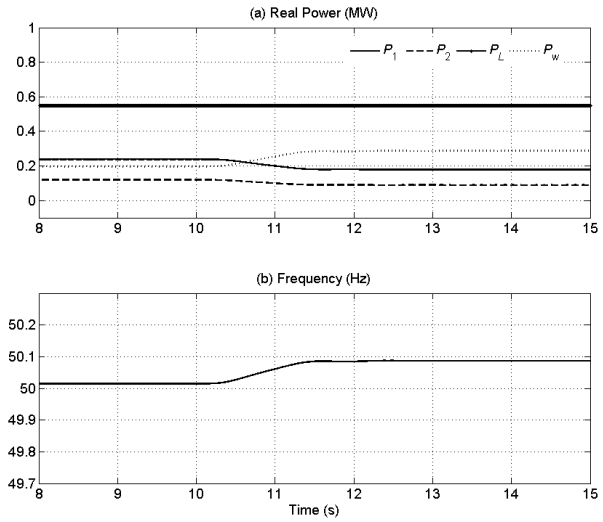

Fig. 18. Real power sharing and frequency of microgrid in Case (c.2).

VI. CONCLUSIONS

In this paper, Optimal Power Control (OPC) scheme is used for MPPT control to draw maximum possible power from the WECS. The WECS is connected through a back to back converter to supply the available maximum power to the microgrid. Two different techniques of WECS integration to the microgrid are proposed in this paper. The microgrid operates in frequency droop control. In the first technique, an isochronization method is used in which the droop line is shifted such that each DG supplies its required power at 50 Hz. This has been discussed in details. The other technique is to synchronize WECS at the microgrid frequency. A simple synchronization method is proposed in which only measurements of the instantaneous PCC voltages are needed. Both these two proposed techniques are validated through computer simulation using PSCAD/EMTDC. It has been shown that both of them work satisfactorily during load change, WECS connection or disconnection with the microgrid. The operation is seamless where no large transient is visible.

ACKNOWLEDGEMENT

The authors thank the Australian Research Council (ARC) for the financial support for this project through the ARC Discovery Grant DP110104554.

REFERENCES

[1] H. Farhangi, "The Path of the Smart Grid ," *IEEE power & energy magazine*, vol.8, no.1, pp.18-28, January-February 2010.

[2] R. Hunter, and G. Elliot, *Wind-Diesel Systems, A Guide to the Technology and its Implementation*. Cambridge, U.K.: Cambridge Univ. Press, 2005.

[3] S. Hier, *Grid Integration of Wind Energy Conversion Systems*, John Wiley and sons, June 2014.

[4] C. Abbey, F. Katiraei, C. Brothers, L. B. Dignard, G. Joos, "Integration of distributed generation and wind energy in Canada," *IEEE, Power Engineering Society General Meeting*, 2006.

[5] N.H. Lipman, "Overview of wind/diesel systems" *Renewable Energy* vol.5, no.1, pp.595-617, August 1994.

[6] F. Katiraei, C. Abbey, "Diesel Plant Sizing and Performance Analysis of a Remote Wind-Diesel Microgrid," *IEEE, Power Engineering Society General Meeting*, pp.1-8, June 2007.

[7] M. Fazeli, G. M. Asher, C. Klumpner, Y. Liangzhong, and M. Bazargan, "Novel Integration of Wind Generator-Energy Storage Systems Within Microgrids," *IEEE Transactions on Smart Grid*, vol.3, no.2, pp.728-737, June 2012.

[8] I. D. Margaris, S.A. Papathanassiou, N.D. Hatziargyriou, A.D. Hansen, and P. Sorensen, "Frequency Control in Autonomous Power Systems With High Wind Power Penetration," *IEEE Transactions on Sustainable Energy*, vol.3, no.2, pp.189-199, April 2012.

[9] E. Planas, A. G. Muro, J. Andreu, I. Kortabarria, and I. M. Alegria, "General aspects, hierarchical controls and droop methods in microgrids : A review," *Renewable and Sustainable Energy Reviews*, vol. 17, pp. 147–159, January 2013.

[10] J.A. P. Lopes, C. L. Moreira, and A.G. Madureira, "Defining control strategies for Microgrids islanded operation," *IEEE Transactions on Power Systems*, vol.21, no.2, pp.916–924, May 2006.

[11] T.L. Vandoorn, B. Meersman, J.D.M. De Kooning, and L. Vandevelde, "Analogy Between Conventional Grid Control and Islanded Microgrid Control Based on a Global DC-Link Voltage Droop," *IEEE Transactions on Power Delivery, ,* vol.27, no.3, pp.1405–1414, July 2012.

[12] A. Mohd, E. Ortjohann, W. Sinsukthavorn, M. Lingemann, N. Hamsic, and D. Morton, "Isochronous load sharing and control for inverter-based distributed generation," *International Conference on Clean Electrical Power, 2009* , pp.324-329, June 2009.

[13] K.J Bunker, and W.W. Weaver, "Microgrid frequency regulation using wind turbine controls," *Power and Energy Conference at Illinois (PECI),* pp.1-6, Feb.-Mar. 2014.

[14] M. R . Patel, *Wind and Solar Power Systems*, USA: CRC Press, 1999, pp. 124-130.

[15] A. A. Jadallah, D. Y. Mahmood, and Z. A. Abdulqader, "Optimal performance of horizontal axis wind turbine for low wind speed regime," *International Journal of Multidisciplinary and Current Research*, vol.2, pp. 159-164, 2014.

[16] J. G. Slootweg, H. Polinder, and W. L. Kling, "Dynamic Modeling of wind turbine with doubly feed induction generator," *IEEE Power Engineering society Summer Meeting*, pp.644-649, July 2001.

[17] K. Kurohane, T. Senjyu, A. Yona, N. Urasaki, T. Goya, and T. Funabashi, "A hybrid smart AC/DC power system," *IEEE Trans. Smart Grid*, vol. 1, no. 2, pp. 199-204, 2010.

[18] B. Wu, Y. Lang, N. Zargari and S. Kouro, *Power Conversion and Control of Wind Energy Systems*, *IEEE* John Wiley and sons, 2011.

[19] A. Ghosh, "Performance study of two different compensating devices in a custom power park," *Proc. IEE, Generation, Transmission & Distribution*, Vol. 152, No. 4, pp. 521-528, 2005.

[20] M. Goyal and A. Ghosh, "A phase-locked-loop design for smooth operation of a hybrid microgrid," *Australasian Universities Power Engineering Conference AUPEC 2013*, Hobart, 2013.

[21] W. V. Lyon, *Transient analysis of alternating-current machinery*, John Wiley, USA, 1954.

APPENDIX

TABLE I. WIND TURBINE AND PMSG PARAMETERS

Parameters Names	Parameter Values
Rotor radius	58 cm
Air density	1.225 kg/m^3
Rated wind speed	12 m/s
Rated apparent power	0.5 MVA
Rated line-to-line voltage	11 kV
Rated frequency	10 Hz
Number of pole pairs	49

TABLE II. PARAMETERS OF THE DGS CONNECTED IN MICROGRID

System Quantities	Values
DG_1 Feeder impedance	R_{f1} = 3.025 Ω, L_{f1} = 57.8 mH
DG_2 Feeder impedance	R_{f2} = 3.025 Ω, L_{f2} = 57.8 mH
DGs Rated Power	DGEN-1: 500 kW, DGEN-2: 250 kW
Droop Coefficient (Frequency–Voltage)	
m_1	0.0075 rad/MWs
m_2	0.015 rad/kWs
n_1	0.02 kV/MVAr
n_2	0.04 kV/MVAr

TABLE III. DIESEL GENERATOR SET DATA

System data	Value
Rated voltage	11 kV
Rated power DGEN1	250 kW
Rated power DGEN2	500 kW
Rated frequency	50Hz
Rated speed	1500 rpm
Reactance	**Value (per unit)**
X_d : Unsaturated *d* axis synchronous reactance	0.116
X'_d : Unsaturated *d* axis transient synchronous reactance	7.4×10^{-3}
X''_d : Unsaturated *d* axis subtransient synchronous	2.94×10^{-3}
X_q : Unsaturated *q* axis synchronous reactance	6.37×10^{-3}
X''_q : Unsaturated *q* axis subtransient synchronous reactance	5.24×10^{-3}
X_2 : Negative-sequence reactance	0.044
X_0 : Zero-sequence reactance	2.45×10^{-3}
Time constants	**Value (ms)**
t''_{do} : *d* axis subtransient open circuit time constant	25

t''_{qo} : q axis subtransient open circuit time constant	4
t'_{d0} : d axis transient open circuit time constant	368
t_a : Armature time constant	25

Table IV. PARAMETERS OF THE ISOCHRONIZATION (PID) CONTROLLER

System data	**Value**
Proportional gain (K_{Pi})	0.1
Integral gain (K_{Ii})	10
Constant coefficient (a)	200